The IS/OS Junction Layer in the Natural History of Type 2 Idiopathic Macular Telangiectasia

Ferenc B. Sallo,[1–3] *Tunde Peto,*[4] *Catherine Egan,*[1] *Ute E. K. Wolf-Schnurrbusch,*[3] *Traci E. Clemons,*[5] *Mark C. Gillies,*[6] *Daniel Pauleikhoff,*[7] *Gary S. Rubin,*[2] *Emily Y. Chew,*[8] *Alan C. Bird,*[9] *and the MacTel Study Group*[10]

Purpose. To document the progression of a break in the photoreceptor inner segment/outer segment (IS/OS) junction layer and its functional correlates over time in the natural history of type 2 idiopathic macular telangiectasia (type 2 MacTel).

Methods. Patients with at least 1 year of follow-up were selected from the MacTel Study. En face images were created by manual segmentation of the IS/OS junctional line in volume scans acquired using a spatial-domain optical coherence tomography retinal imaging unit. Retinal sensitivity thresholds were determined using a retinal microperimeter unit. Aggregate retinal sensitivity loss within IS/OS lesions was calculated. Changes over time in an area of IS/OS defects and retinal sensitivity were analyzed.

Results. Thirty-nine eyes of 23 patients (mean age: 62.3 ± 9.2 years) were analyzed. Mean follow-up time was 1.9 years (range: 1–3 years). Mean IS/OS break area at baseline was 0.575 mm^2 (SE = 0.092, 95% confidence interval [CI]: 0.394–0.756 mm^2). The cluster-adjusted mean annual progression rate in IS/OS break area was 0.140 mm^2 (SE = 0.040, 95% CI: 0.062–0.218 mm^2, $P < 0.001$). Mean aggregate retinal sensitivity loss was at baseline 28.56 dB (SE = 5.43, 95% CI: 17.32–39.80 dB, $n = 28$), a positive correlation with IS/OS lesion area was present ($P < 0.001$). The mean annual rate of change in aggregate sensitivity loss was 5.14 dB (SE = 1.51, 95% CI: 2.19–8.10 dB, $P < 0.001$, $n = 37$), a significant correlation with lesion area increase was found ($P = 0.006$).

Conclusions. Both IS/OS break area and rate of enlargement correlate with aggregate retinal sensitivity loss in type 2 MacTel. En face OCT imaging of the IS/OS layer provides a functionally relevant method for documenting disease progression in type 2 MacTel. (*Invest Ophthalmol Vis Sci.* 2012; 53:7889–7895) DOI:10.1167/iovs.12-10765

Type 2 Idiopathic Macular Telangiectasia (type 2 MacTel) is a retinal disease that affects the juxtafoveal region of both eyes.[1,2] The etiology and pathogenesis of the disease are unknown and no proven treatment is currently available.

The diagnosis of type 2 MacTel is based on stereoscopic biomicroscopic and fundus fluorescein angiographic (FFA) observations, including a loss of retinal transparency; dilated, blunted, and right-angled veins; dilated capillaries and telangiectatic vessels in the deep retinal plexus; hyperfluorescence in the angiogram without cystoid edema; and pigment plaques. Fibrosis accompanied by eventual neovascularization, scarring, and atrophy are associated with a loss of visual acuity. Early clinical signs may be quite subtle and challenging to quantify.

The introduction of optical coherence tomography (OCT) imaging has provided a valuable tool for identifying neurodegenerative changes in type 2 MacTel. An overall thinning of the retinal temporal to the foveal center, a deformation of the foveal contour, hyporeflective spaces in the inner and outer retina, and a break in the line considered to represent the junctions between the photoreceptor inner and outer segments (IS/OS line)[3–6] are commonly found. Disruption of the IS/OS line has been demonstrated to correlate with retinal function loss in several retinal disorders[5,7–25] and is considered a useful indicator of photoreceptor integrity and predictor of visual function.

In a previous study we demonstrated that imaging the IS/OS layer en face (in the coronal plane) provides a functionally relevant method for quantifying the extent of outer retinal abnormalities as well as for assessing their topographic relationships in type 2 MacTel.[26]

The aim of the present study was to document the progression of the abnormalities of the IS/OS layer and retinal function over time using en face spectral domain (SD)-OCT imaging and mesopic microperimetry.

Methods

Patients

Thirty-nine eyes of 23 patients, ranging in age at baseline from 46 to 76 years (mean = 62.3 years, SD = 9.2 years; 11 males, 12 females), were

From the [1]Department of Research and Development, Moorfields Eye Hospital, London, United Kingdom; the [2]University College London (UCL) Institute of Opthalmology, London, United Kingdom; the [3]Universtätsklinik fül Augenheilkunde, University of Bern, Bern, Switzerland; the [4]National Institute for Health Research Biomedical Research Centre for Ophthalmology, at Moorfields Eye Hospital National Health Service Foundation Trust and UCL Institute of Ophthalmology, London, United Kingdom; the [5]EMMES Corporation, Rockville, Maryland; the [6]Save Sight Institute, University of Sydney, Sydney, Australia; the [7]St. Franziskus Hospital, Münster, Germany; and the [8]National Eye Institute, National Institutes of Health, Bethesda, Maryland; and the [9]Division of Inherited Eye Disease, Moorfields Eye Hospital, London, United Kingdom.

[10]See the Appendix for the Participating Principal Investigators and Centers in the MacTel Study Group.

Supported by the Lowy Medical Research Institute (LMRI) and the National Institute for Health Research. The LMRI also participated in the design of the study and in the review and approval of the manuscript.

Submitted for publication August 14, 2012; accepted October 19, 2012.

Disclosure: **F.B. Sallo**, None; **T. Peto**, None; **C. Egan**, None; **U.E.K. Wolf-Schnurrbusch**, None; **T.E. Clemons**, None; **M.C. Gillies**, None; **D. Pauleikhoff**, None; **G.S. Rubin**, None; **E.Y. Chew**, None; **A.C. Bird**, None

Corresponding author: Ferenc B. Sallo, The Reading Centre, Department of Research and Development, Moorfields Eye Hospital NHS Foundation Trust, 162 City Road, London, EC1V 2PD, UK; Ferenc.Sallo@moorfields.nhs.uk.

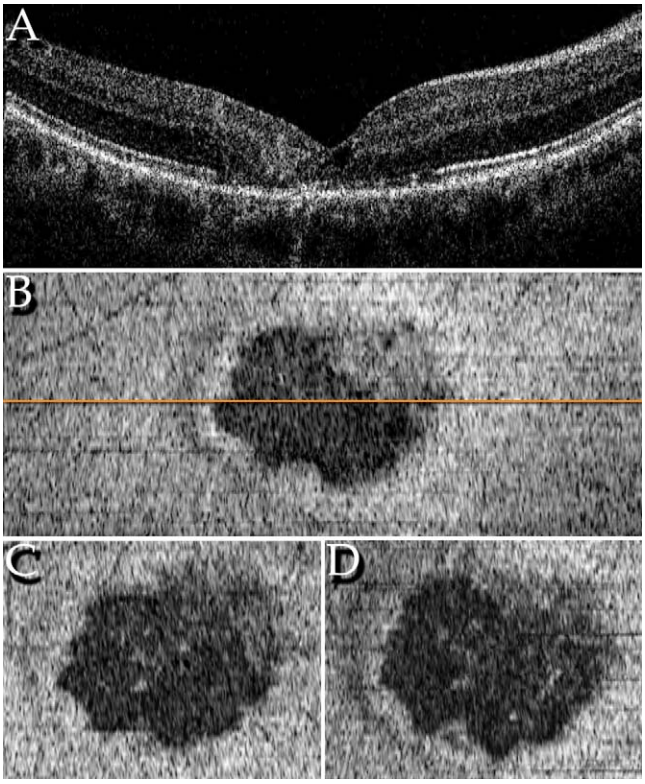

Figure 1. The IS/OS lesion en face and corresponding B-scan, progression of the lesion size, and structure over time. (**A**) Sample B-scan of a type 2 MacTel eye; an *orange line* marks its location within the en face image in (**B**). In (**A**), note the sharp boundary on the *left edge* and the irregular attenuation of the IS/OS line on the *right side*, corresponding within the en face image to a distinct boundary in the *left* and inferior part and a gradual, patchy thinning in the superior and *right* part of the break, respectively. (**B**) Within the en face image, the IS/OS break appears as a *darker area* against the background of the highly reflective IS/OS layer. Internal to the edges of the lesion areas with a reflectivity similar to that of the IS/OS are also apparent. These may correspond to islands of preserved IS/OS, but more frequently to the cross-section of an area with pathologic vertical restructuring of the retina where retinal layers between the outer plexiform layer and the RPE seem to be absent and the disorganized outer plexiform layer and layers interior to it give the impression of "collapsing" onto the RPE (see [**A**]). (**B–D**) En face images from 2007, 2009, and 2011. Progression in area occurs both along the distinct edge as well as through gradual thinning of the IS/OS (*top right edge*). "Collapsed" layers in cross-section appear to increase in area as well as optical density. RPE, retinal pigment epithelium.

examined. Mean follow-up time was 1.9 years (SD = 0.6 years; range: 1–3 years). Patients were selected from the cohort of the MacTel project, an international multicenter prospective natural history study of type 2 MacTel, currently involving 27 research centers worldwide.[27] Eyes of participants from one site within the study with at least 1 year of follow-up and available SD-OCT volume scans, demonstrating a break in the IS/OS line at baseline were included. Treated eyes and eyes containing dense pigment plaques obscuring the deeper layers of the retina or showing signs of neovascularization at baseline were excluded. The study protocol adhered to the tenets of the Declaration of Helsinki and was approved by the local institutional ethics committee. Written, informed consent was obtained from each participant after explanation of the nature of the study.

Imaging

Standard 30° stereo field 2 color (CF) and red-free (RF) images of the fundus were recorded digitally. SD-OCT volume scans consisting of 128 B-scans within a 6 × 6-mm retinal area, with a resolution of 512 A-scans per B-scan, were acquired using an SD-OCT retinal imaging unit (Topcon 3D-OCT1000; Topcon Medical Systems, Inc., Oakland, NJ).

A total of 105 OCT volume scans were processed. The Topcon Q factor (reflecting signal strength) ranged from 30.12 to 83.54 (mean = 57.50, SE = 1.44 95% confidence interval [CI]: 54.68–60.32). Motion artifacts due to microsaccades and/or drift parallel to the B-scans present in 11 volume scans were corrected. Six scans with incorrigible motion artifacts (e.g., where disparate retinal areas were scanned into a volume due to microsaccades with a vector at an angle to the direction of the B-scans) were discarded. Uneven field illumination was noted in 7 scans.

SD-OCT Image Processing

The procedure used in this study for creating and processing en face images has been described previously.[26] Briefly, the IS/OS line was segmented manually, using dedicated 3D image-analysis software (Visage Imaging Amira v5.3.3; Pro Medicus Ltd., Richmond, Victoria, Australia); en face images exported in grayscale using orthogonal projection were resampled using an image editing program (Adobe Photoshop CS5 Extended; Adobe Systems Inc., San Jose, CA); a 3 × 3 pixel normal filter was applied to reduce noise emanating from high-frequency random variation and from slight misalignments and variation in reflectivity between individual B-scans within the SD-OCT volume. Delineation of the IS/OS lesions was performed manually. The IS/OS break area and the radial distance of the nearest lesion edge from the anatomic center of the fovea were measured, expressed in pixels.

Functional Testing

Monocular best-corrected visual acuities (BCVAs) were determined according to a standardized protocol, using Early Treatment Diabetic Retinopathy Study visual acuity charts at a distance of 4 meters. Scoring of the test was based on the number of letters read correctly. Possible scores ranged from 0 (Snellen equivalent < 20/800) to 100 (Snellen equivalent 20/12).[28,29] Fundus-correlated automated microperimetry was performed using a retinal microperimeter unit (Nidek MP1 and Navis software version 1.7.3; Nidek Technologies, Albignasego, Italy), following pupil dilatation with 1.0% tropicamide (Mydriacyl Eye Drops; Tocris Bioscience, Bristol, UK) and 2.5% phenylephrine hydrochloride and 5 minutes of visual dark adaptation. The technique has been described previously.[26,30–32] Results are reported in decibels.

Data Analysis

An approximate calibration of distances within the en face OCT image to metric units was performed based on the uniform 6-mm width of the scan raster. En face SD-OCT images and microperimetric retinal sensitivity threshold data were superimposed over images of the fundus and adjusted to attain exact correspondence. To reduce bias from conditions unrelated to MacTel,[27] only microperimetric data from test points within the central 10° of the MP1 grid were considered in calculations. For assessing change over time in retinal function, aggregate sensitivity loss was calculated: The mean of retinal sensitivity values measured within the central 10° of the grid at test points not within the area of the IS/OS break was calculated and considered the background sensitivity. Aggregate loss was defined as the sum of deviations from the background sensitivity of values measured at test points within the area of the IS/OS break. Annual rate of change in the lesion area and aggregate loss were calculated and compared.

Statistical Methods

A value of $P < 0.05$ was accepted as statistically significant. Since some participants in this cohort have both eyes included (clustered data), analytic methods accounting for the correlation between eyes

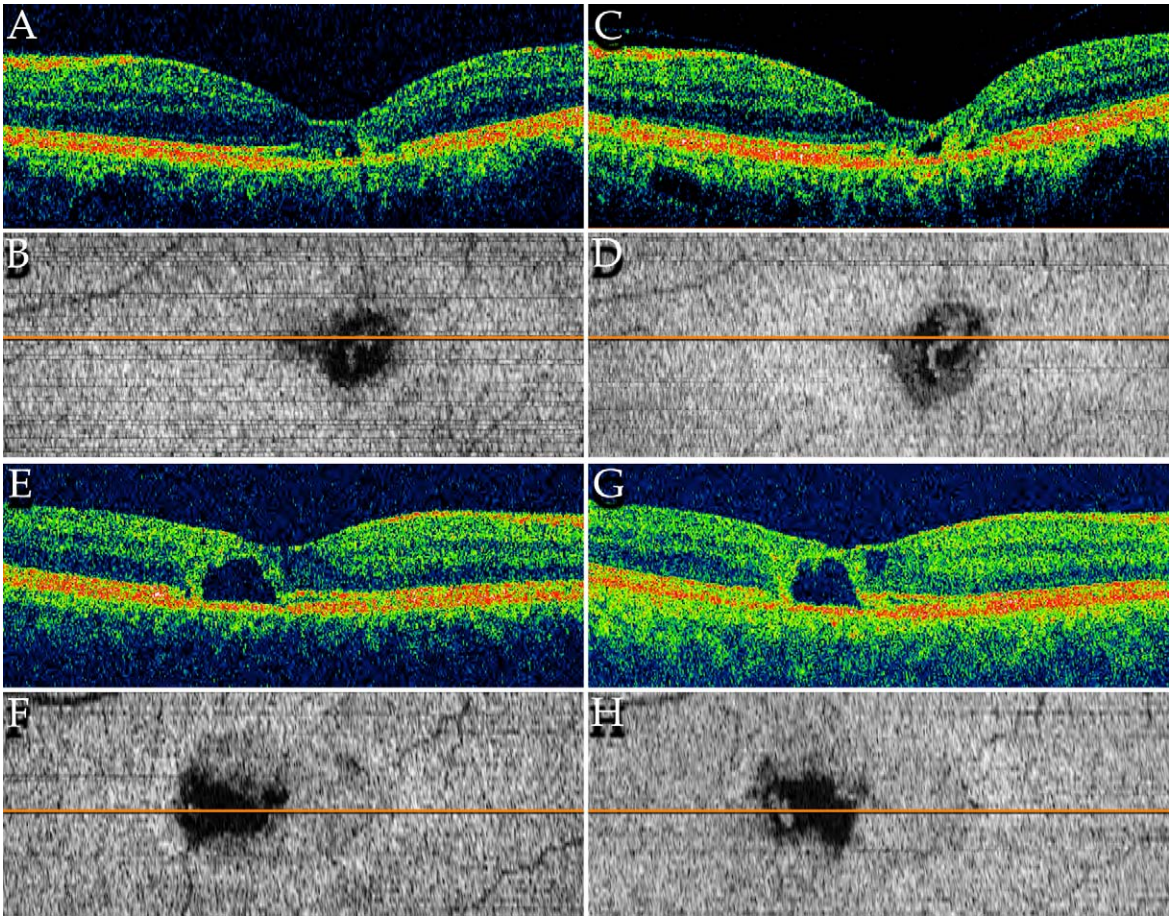

Figure 2. Progression of the IS/OS break in 2 years. Within the area of the IS/OS break, insular variations of backscatter may be present. Low optical density corresponds to the cross-sections of outer retinal atrophic cavities, a high reflectivity to cross-sections of an abnormal retinal tissue with a vertical orientation. In these, retinal layers between the outer plexiform layer and the RPE seem to be absent and the structurally disorganized remaining retinal layers give the impression of "collapsing" onto the RPE. This structure was always seen initially on the temporal side of the foveal center.[3,6] Islands of preserved IS/OS may also present as areas with high reflectivity. Images on the *left* were taken in 2008, on the *right* in 2010. *Orange lines* mark the position of respective B-scan within the en face image. (**B**, **D**) In the en face images, a significant increase in break area is accompanied by a reduction in the area of the cross-sections of the outer retinal empty spaces (*near-black areas*) and the enlargement of a highly reflective area corresponding in B-scans (**A**, **C**) to outer retinal atrophy and a pathologic vertical restructuring of the retina. (**F**, **H**) Although the overall increase in the break area is minor, the progression of retinal restructuring is detectable in the en face image, the shape of the outer empty space changes, and the area and optical density of the collapsed layers increase (compare with [**E**] and [**G**]).

(marginal generalized estimating equations [GEE]) were used.[33] In the GEE, dependence within clusters is treated as a nuisance parameter and inferences are predicted for population average effects. The least-square means, SEs, and 95% CI values from the models are provided. All analyses were conducted using commercially available statistical software (SAS version 9.02; SAS Institute, Cary, NC).

Results

Phenotype

Mean area of the IS/OS break accounting for correlation between eyes for those participants with two eyes at baseline was 0.575 mm^2 (SE = 0.092, 95% CI: 0.394–0.756 mm^2). The cluster-adjusted mean annual progression rate in the area of IS/OS break was 0.140 mm^2 (SE = 0.040, 95% CI: 0.062–0.218 mm^2, $P < 0.001$). Concordance of the rate of expansion of the area of disruption between fellow eyes was low ($\rho = -0.20$, $P = 0.46$, concordance correlation coefficient = –0.14, $n = 16$). Expansion was observed both along distinct edges as well as through gradual thinning of the IS/OS (Fig. 1).

Within the area of the lesion, a decrease in size of hyporeflective spaces in the outer retina was observed with a simultaneous increase in thickness and reflectivity of the "collapsed layers," as described in Figures 2B–D. Topographically, the IS/OS break initially located on the temporal side of the fovea progressed in all directions, including toward the foveal center. The IS/OS break affected the foveal center at baseline in 12 of 39 eyes. The rate of expansion in eyes with an affected foveal center at baseline was 0.115 ± 0.023 mm^2 compared with 0.080 ± 0.027 mm^2 in eyes where the foveal center was spared at baseline ($P = 0.31$).

Morphologic signs of abnormality of the IS/OS may be detectable even before a clear break is present. In en face OCT images, a gray area may be a sign of an attenuated backscatter from the IS/OS and may have functional correlates.[34] In our cohort, retinal sensitivity measured in these gray areas was decreased, but the levels of sensitivity loss were well below the pointwise repeatability (5.56 dB) for MP1 testing.[35] The signal from the IS/OS may also be normal in intensity but abnormal in its location. This presents most frequently as a depression within the fovea externa (Fig. 3). These signs may also accompany manifest breaks.

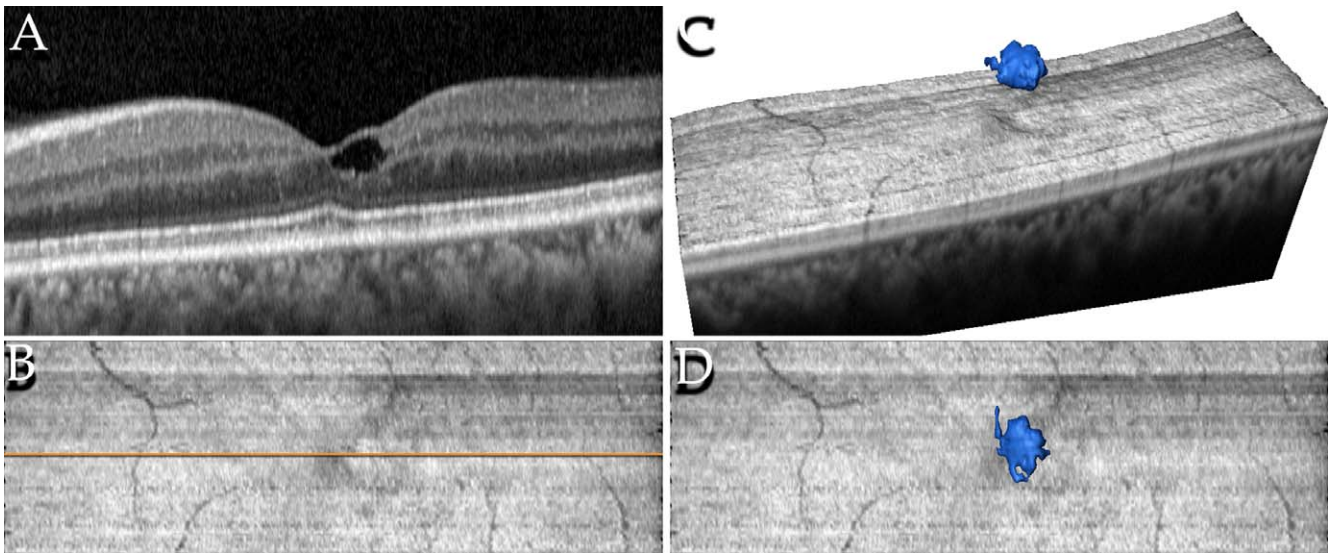

Figure 3. Abnormal shape of the IS/OS junction layer without a manifest break. OCT images of a type 2 MacTel eye. (**A**) B-scan showing a large inner retinal cyst with signs of elevated internal pressure, deforming the surface contour of the retina. The IPL is laterally displaced; the OPL, ONL, external limiting membrane, and IS/OS line deviate toward the RPE within the area of the fovea interna, in line with the cyst. (**B**) With respect to the en face image of the IS/OS layer, a break is not detectable. An irregular area around the foveal center shows attenuated backscatter. An *orange line* marks the position of the B-scan in (**A**). (**D**) The volume of the inner retinal cyst (rendered in *blue*), superimposed over the en face image. (**C**) 3D perspective view of the IS/OS layer and the inner cyst, a large part of the fovea interna is sunken toward the RPE; this corresponds directly to the location of the cyst. A similar deformation of the IS/OS may also accompany an IS/OS break. (*Darker horizontal striping* is due to an artifactual variation in B-scan intensity.)

Functional Testing

The mean BCVA at baseline was 71 letters (Snellen equivalent 20/36, SE = 2.02 letters, 95% CI: 67–75 letters, $n = 39$). Mean yearly loss was 0.267 letters (SE = 0.591 letters, 95% CI: −1.43 to 0.89 letters, $P = 0.65$). From a generalized linear model (GLM) accounting for clustering, the relationship with the annual rate of change in the area of disruption did not meet statistical significance (regression model = 0.115 + 0.032 × [annual rate of change in BCVA]; P value for slope = 0.19). The slope, interpreted as an increase for each unit annual rate of change in BCVA, is associated with an estimated increase of 0.032 mm^2 in the mean annual rate of change in area of disruption.

Mean aggregate MP1 retinal sensitivity loss at baseline was 28.56 dB (SE = 5.43, 95% CI: 17.32–39.80 dB, $n = 28$). From a GLM the model was computed as 0.183 + 0.013 × [MP1 retinal sensitivity], with a P value for the slope of <0.001. The slope, interpreted as an increase of 1 dB in baseline MP1 retinal sensitivity loss, is associated with an estimated increase of 0.013 mm^2 in the mean baseline IS/OS break measurement. The mean annual rate of change in aggregate sensitivity loss was 5.14 dB (SE = 1.51, 95% CI: 2.19–8.10 dB, $P < 0.001$, $n = 37$). From a GLM accounting for clustering, the relationship with the annual rate of change in the area of disruption met statistical significance (regression model = 0.079 + 0.006 × [MP1 aggregate retinal sensitivity loss annual rate of change]; P value for slope = 0.006). The slope, interpreted as an increase for each unit annual rate of change in MP1 aggregate retinal sensitivity loss annual rate of change, is associated with an estimated increase of 0.006 mm^2 in the mean annual rate of change in the area of disruption.

Discussion

We undertook this study to identify a sensitive, functionally relevant outcome to monitor progression of type 2 MacTel. Visual acuity is a poor measure since the disease may become advanced in the perifoveal region without affecting visual acuity. Microperimetry is a functional measure, but it is subjective. We have demonstrated in this study that en face imaging of the area of IS/OS disruption correlates strongly with loss of macular sensitivity measured by microperimetry, and that expansion of the area of photoreceptor dysfunction correlates with progressive loss of macular sensitivity. En face imaging of the area of the IS/OS break may therefore be considered as an outcome measure for clinical trials of interventions for type 2 MacTel.

The main change over time in the morphology of a manifest break in the IS/OS junction layer is an increase in its area. This was observed both by progression of distinct edges as well as a gradual diffuse fading over a larger area (Fig. 1). The mean annual increase in area of 0.140 mm^2 in our cohort was easily detectable at the currently available resolution of the en face images. An outright recovery of a clear IS/OS break was not seen, although a variation between scans in break shape was noted, possibly due to the optical properties of the layer or the OCT system used. We previously found variation in break area size between fellow eyes to be smaller than that between patients.[26] However, a similar significant symmetry between left and right eyes of the increase in IS/OS area over time could not be demonstrated in this cohort. This may be attributable to the relatively short follow-up time in this study.

We found a significant and close correlation between area size of an IS/OS break and aggregate mesopic retinal sensitivity loss. Furthermore, an enlargement of the break area over time was associated with an increase in aggregate sensitivity loss, although the correlation of break area change with BCVA was not significant.

Within the area of the break, cross-sections of outer retinal cavities, islands of preserved IS/OS, or cross-sections of an abnormal retinal tissue with a vertical orientation may be present ("collapsed layers"; see Fig. 2). These features are

Figure 4. Focal lateral contraction of the retina temporal of the foveal center in type 2 MacTel. (**A**) In 2008, in an early-phase FA image, dilated veins from the superior and inferior temporal branches and a dilated deep capillary plexus are evident. (**B**) By 2010, pigment appears, the retina around it contracts, radial vessels straighten, and point toward the tissue surrounding the pigment deposit. (**C**) The tissue corresponds in the en face OCT image to the cross-section of "collapsed" layers.

smaller and some are scattered and indistinct, such that their changes over time are not amenable to accurate quantification. However, as a trend it was noted that an increase in break area was often accompanied by a progression of retinal restructuring ("collapsed layers"), with a simultaneous overall decrease of the adjacent outer atrophic spaces.

Based on our own and previous observations by other authors[3,6,25] a hypothetical sequence of neurodegenerative signs in MacTel may be outlined: Inner hyporeflective spaces near the foveal center appear, initially convex both anteriorly and posteriorly, distending the retina, the IS/OS junction layer deviates toward the retinal pigment epithelium (RPE) (Fig. 3A). Subsequently, the convexity disappears, leaving the impression of an inner atrophic cavity (Figs. 2G, 5A). Minor vertically oriented oblong spaces along the border of the outer nuclear and outer plexiform layers (OPL and ONL) may also be present. Temporal to the foveal center, the IS/OS signal attenuates and breaks and outer retinal spaces appear, with a shape suggesting atrophy (lateral boundaries in B-scans near the RPE appear vertical, in line with photoreceptor morphology). Focally, the ONL thickness decreases, layers internal to the ONL deviate toward the RPE/choroid, become disorganized, and "collapse" onto the RPE. As the collapse widens, outer empty spaces shrink. Some authors characterize the "collapse" as a "contraction" of retinal layers.[5] Indeed, a contraction in the plane of the retina centered on these foci is frequently seen in fundus images (see Fig. 4), along with apparent anastomoses between branches of the supero- and inferotemporal venous systems. A vertical component is also conceivable. We noted in en face images that the cross-section of the collapsed tissue often colocalized with the tips of blunted veins in the fundus image (Fig. 5). We were unable to clearly demonstrate blood vessels within the collapsing layers, possibly due to the relatively low resolution of the en face images. However, aberrant blood vessels within the outer retina, near the foveal center, have been reported previously,[25,36] and vascular involvement in the "collapse" is possible. Although the pigment plaques characteristic of type 2 MacTel are in the mid layers of the retina, smaller foci were observed in the deeper layers of the retina also in this cohort. Vessels with a vertical disposition combined with the propensity of pigment for propagating along vessels[37] may offer an explanation for pigment plaque genesis. Progression of the phenotype, however, may not necessarily always pass through the same sequence of events in all cases.

We acknowledge some limitations of this study. Sample size and follow-up time were limited. For an accurate calibration of measurements within OCT images, the axial length and the refractive power of the eye must be taken into consideration. In our study these data were not collected; "typical" values were used as provided by the manufacturer. However, we compared each individual eye over time in terms of structure and function. Unless there is a significant change in the main

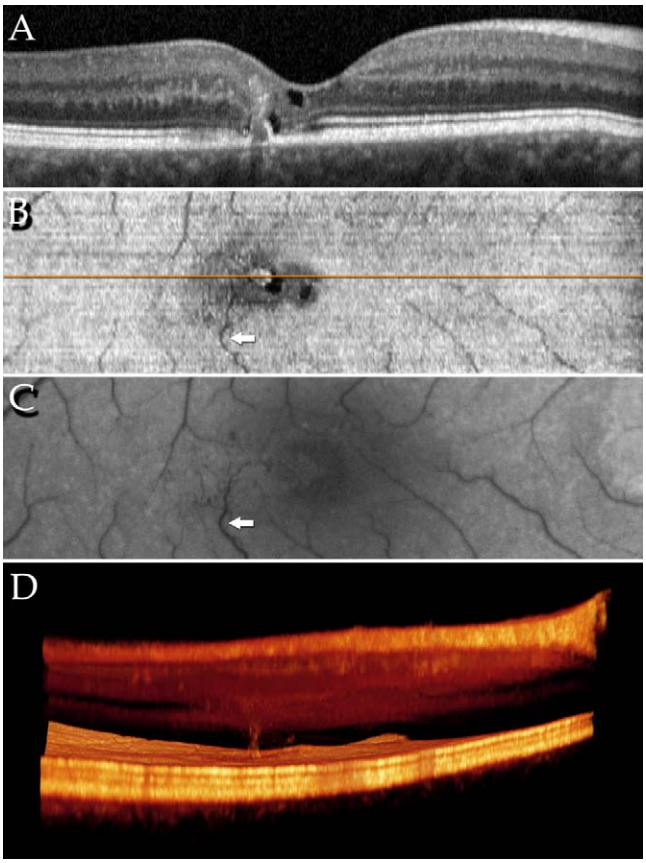

Figure 5. "Collapsed" retinal layers with indications of vascular involvement. (**A**) B-scan OCT image. (**B**) OCT en face image of the IS/OS junction layer; an *orange line* marks the location of the B-scan in image (**A**); a *white arrow* marks a dilated vein. (**C**) Red-free image of the same retinal location. The cross-section of the collapsing layers colocalizes with the tip of a dilated vein (*arrow*) that changes caliber abruptly. (**D**) 3D perspective rendering of the OCT data; note the sunken appearance of the IS/OS layer around the break in the temporal part of the fovea externa and the vertical, optically dense tissue extending between the inner and outer layers.

parameters (due to, e.g., cataract or refractive surgery, a change in the refractive index of the lens due to maturing cataract, or an increase in axial length in progressive myopia), differences in area measured are expected to emanate from the progression of the lesion alone. The low test point density of the MP1 grid used did not permit a detailed analysis of whether function loss is associated with the IS/OS break itself or lesions within. It was noted, however, that high loss was consistently present over "collapsed layers." A progression of the collapsing layers may have a functional relevance that would not be fully reflected in increasing lesion area size alone. Furthermore, we used volume scans from a commercially available SD-OCT machine without a real-time eye-tracking system. Fixation stability in type 2 MacTel patients is affected early and motion artifacts may be a source of error in 3D analysis. In en face images, near the foveal center, in the absence of vascular landmarks, it may not always be possible to detect these. OCT devices with active eye tracking have a significant advantage.

SD-OCT and other recent imaging techniques offer possibilities for characterizing the neurodegenerative aspects of the disease[3,5,6,25,38,39] and may provide new morphologic landmarks for refining the staging system, especially in early disease.[40] Break area in en face images of the IS/OS layer is a quantifiable morphologic sign that correlates with function also in its progression over time, even at stages of the disease where vascular signs may be less sensitive indicators. The IS/OS break and "collapsing tissue" may potentially be new landmarks for following disease progression in the natural history as well as in interventional studies of MacTel.

Acknowledgments

The authors thank Austin Roorda for valuable discussions concerning the optical properties of the retina and Marcus Fruttiger for valuable discussions concerning microanatomic, histologic, and cell biological aspects of type 2 MacTel.

References

1. Gass JD, Oyakawa RT. Idiopathic juxtafoveolar retinal telangiectasis. *Arch Ophthalmol*. 1982;100:769–780.
2. Gass JD, Blodi BA. Idiopathic juxtafoveolar retinal telangiectasis. Update of classification and follow-up study. *Ophthalmology*. 1993;100:1536–1546.
3. Gaudric A, Ducos de Lahitte G, Cohen SY, Massin P, Haouchine B. Optical coherence tomography in group 2A idiopathic juxtafoveolar retinal telangiectasis. *Arch Ophthalmol*. 2006; 124:1410–1419.
4. Yannuzzi LA, Bardal AM, Freund KB, Chen KJ, Eandi CM, Blodi B. Idiopathic macular telangiectasia. *Arch Ophthalmol*. 2006; 124:450–460.
5. Maruko I, Iida T, Sekiryu T, Fujiwara T. Early morphological changes and functional abnormalities in group 2A idiopathic juxtafoveolar retinal telangiectasis using spectral domain optical coherence tomography and microperimetry. *Br J Ophthalmol*. 2008;92:1488–1491.
6. Krivosic V, Tadayoni R, Massin P, Erginay A, Gaudric A. Spectral domain optical coherence tomography in type 2 idiopathic perifoveal telangiectasia. *Ophthalmic Surg Lasers Imaging*. 2009;40:379–384.
7. Ota M, Tsujikawa A, Murakami T, et al. Foveal photoreceptor layer in eyes with persistent cystoid macular edema associated with branch retinal vein occlusion. *Am J Ophthalmol*. 2008; 145:273–280.
8. Shin HJ, Chung H, Kim HC. Association between integrity of foveal photoreceptor layer and visual outcome in retinal vein occlusion. *Acta Ophthalmol*. 2011;89:e35–e40.
9. Maheshwary AS, Oster SF, Yuson RM, Cheng L, Mojana F, Freeman WR. The association between percent disruption of the photoreceptor inner segment-outer segment junction and visual acuity in diabetic macular edema. *Am J Ophthalmol*. 2010;150:63–67.
10. Rangaswamy NV, Patel HM, Locke KG, Hood DC, Birch DG. A comparison of visual field sensitivity to photoreceptor thickness in retinitis pigmentosa. *Invest Ophthalmol Vis Sci*. 2010;51:4213–4219.
11. Aizawa S, Mitamura Y, Baba T, Hagiwara A, Ogata K, Yamamoto S. Correlation between visual function and photoreceptor inner/outer segment junction in patients with retinitis pigmentosa. *Eye*. 2009;23:304–308.
12. Ergun E, Hermann B, Wirtitsch M, et al. Assessment of central visual function in Stargardt's disease/fundus flavimaculatus with ultrahigh-resolution optical coherence tomography. *Invest Ophthalmol Vis Sci*. 2005;46:310–316.
13. Park SJ, Woo SJ, Park KH, Hwang JM, Chung H. Morphologic photoreceptor abnormality in occult macular dystrophy on spectral-domain optical coherence tomography. *Invest Ophthalmol Vis Sci*. 2010;51:3673–3679.
14. Kim YG, Baek SH, Moon SW, Lee HK, Kim US. Analysis of spectral domain optical coherence tomography findings in occult macular dystrophy. *Acta Ophthalmol*. 2011;89:e52–e56.
15. Hayashi H, Yamashiro K, Tsujikawa A, Ota M, Otani A, Yoshimura N. Association between foveal photoreceptor integrity and visual outcome in neovascular age-related macular degeneration. *Am J Ophthalmol*. 2009;148:83–89.
16. Landa G, Su E, Garcia PM, Seiple WH, Rosen RB. Inner segment-outer segment junctional layer integrity and corresponding retinal sensitivity in dry and wet forms of age-related macular degeneration. *Retina*. 2011;31:364–370.
17. Eandi CM, Chung JE, Cardillo-Piccolino F, Spaide RF. Optical coherence tomography in unilateral resolved central serous chorioretinopathy. *Retina*. 2005;25:417–421.
18. Piccolino FC, de la Longrais RR, Ravera G, et al. The foveal photoreceptor layer and visual acuity loss in central serous chorioretinopathy. *Am J Ophthalmol*. 2005;139:87–99.
19. Ojima Y, Hangai M, Sasahara M, et al. Three-dimensional imaging of the foveal photoreceptor layer in central serous chorioretinopathy using high-speed optical coherence tomography. *Ophthalmology*. 2007;114:2197–2207.
20. Ojima Y, Tsujikawa A, Hangai M, et al. Retinal sensitivity measured with the micro perimeter 1 after resolution of central serous chorioretinopathy. *Am J Ophthalmol*. 2008; 146:77–84.
21. Chalam KV, Murthy RK, Gupta SK, Brar VS, Grover S. Foveal structure defined by spectral domain optical coherence tomography correlates with visual function after macular hole surgery. *Eur J Ophthalmol*. 2010;20:572–577.
22. Inoue M, Watanabe Y, Arakawa A, Sato S, Kobayashi S, Kadonosono K. Spectral-domain optical coherence tomography images of inner/outer segment junctions and macular hole surgery outcomes. *Graefes Arch Clin Exp Ophthalmol*. 2009; 247:325–330.
23. Yamauchi Y, Agawa T, Tsukahara R, et al. Correlation between high-resolution optical coherence tomography (OCT) images and histopathology in an iodoacetic acid-induced model of retinal degeneration in rabbits. *Br J Ophthalmol*. 2011;95: 1157–1160.
24. Charbel Issa P, Troeger E, Finger R, Holz FG, Wilke R, Scholl HP. Structure-function correlation of the human central retina. *PLoS ONE*. 2010;5:e12864.
25. Paunescu LA, Ko TH, Duker JS, et al. Idiopathic juxtafoveal retinal telangiectasis: new findings by ultrahigh-resolution optical coherence tomography. *Ophthalmology*. 2006;113:48–57.

26. Sallo FB, Peto T, Egan C, et al. "En face" OCT imaging of the IS/OS junction line in Type 2 idiopathic macular telangiectasia. *Invest Ophthalmol Vis Sci*. 2012;53:6145–6152.
27. Clemons TE, Gillies MC, Chew EY, et al. Baseline characteristics of participants in the natural history study of macular telangiectasia (MacTel) MacTel Project Report No. 2. *Ophthalmic Epidemiol*. 2010;17:66–73.
28. Ferris FL 3rd, Kassoff A, Bresnick GH, Bailey I. New visual acuity charts for clinical research. *Am J Ophthalmol*. 1982;94:91–96.
29. Early Treatment Diabetic Retinopathy Study design and baseline patient characteristics. ETDRS report number 7. *Ophthalmology*. 1991;98:741–756.
30. Rohrschneider K, Springer C, Bultmann S, Volcker HE. Microperimetry—comparison between the micro perimeter 1 and scanning laser ophthalmoscope—fundus perimetry. *Am J Ophthalmol*. 2005;139:125–134.
31. Midena E, Vujosevic S, Convento E, Manfre A, Cavarzeran F, Pilotto E. Microperimetry and fundus autofluorescence in patients with early age-related macular degeneration. *Br J Ophthalmol*. 2007;91:1499–1503.
32. Schmitz-Valckenberg S, Ong EE, Rubin GS, et al. Structural and functional changes over time in MacTel patients. *Retina*. 2009;29:1314–1320.
33. Liang K-Y, Zeger SL. Longitudinal data analysis using generalized linear models. *Biometrika*. 1986;73:13–22.
34. Hood DC, Zhang X, Ramachandran R, et al. The inner segment/outer segment border seen on optical coherence tomography is less intense in patients with diminished cone function. *Invest Ophthalmol Vis Sci*. 2011;52:9703–9709.
35. Chen FK, Patel PJ, Xing W, et al. Test-retest variability of microperimetry using the Nidek MP1 in patients with macular disease. *Invest Ophthalmol Vis Sci*. 2009;50:3464–3472.
36. Green WR, Quigley HA, De la Cruz Z, Cohen B. Parafoveal retinal telangiectasis. Light and electron microscopy studies. *Trans Ophthalmol Soc U K*. 1980;100:162–170.
37. Eliassi-Rad B, Green WR. Histopathologic study of presumed parafoveal telangiectasis. *Retina*. 1999;19:332–335.
38. Zeimer MB, Padge B, Heimes B, Pauleikhoff D. Idiopathic macular telangiectasia type 2: distribution of macular pigment and functional investigations. *Retina*. 2010;30:586–595.
39. Charbel Issa P, Berendschot TT, Staurenghi G, Holz FG, Scholl HP. Confocal blue reflectance imaging in type 2 idiopathic macular telangiectasia. *Invest Ophthalmol Vis Sci*. 2008;49:1172–1177.
40. Wong WT, Forooghian F, Majumdar Z, Bonner RF, Cunningham D, Chew EY. Fundus autofluorescence in type 2 idiopathic macular telangiectasia: correlation with optical coherence tomography and microperimetry. *Am J Ophthalmol*. 2009;148:573–583.

APPENDIX

Participating Principal Investigators and Centers in the MacTel Study

Jose-Alain Sahel, MD, PhD, Centre Hopitalier National d'Ophtalmologie des Quinze-Vingts, Paris, France;
Robyn Guymer, MD, Centre for Eye Research, East Melbourne, Australia;
Gisele Soubrane, MD, PhD, FEBO, Clinique Ophtalmologie de Creteil, Creteil, France;
Alain Gaudric, MD, Hopital Lariboisiere, Paris, France;
Steven Schwartz, MD, Jules Stein Eye Institute, UCLA, Los Angeles, CA (USA);
Ian Constable, MD, Lions Eye Institute, Nedlands, Australia;
Michael Cooney, MD, MBA, Manhattan Eye, Ear, and Throat Hospital, New York, NY (USA);
Catherine Egan, MD, Moorfields Eye Hospital, London, England (UK);
Lawrence Singerman, MD, Retina Associates of Cleveland, Cleveland, OH (USA);
Mark C. Gillies, MD, PhD, Save Sight Institute, Sydney, Australia;
Martin Friedlander, MD, PhD, Scripps Research Institute, La Jolla, CA (USA);
Daniel Pauleikhoff, Prof Dr, St. Franziskus Hospital, Muenster, Germany;
Joseph Moisseiev, MD, The Goldschleger Eye Institute, Tel Hashomer, Israel;
Richard Rosen, MD, The New York Eye and Ear Infirmary, New York, NY (USA);
Robert Murphy, MD, The Retina Group of Washington, Fairfax, VA (USA);
Frank Holz, MD, University of Bonn, Bonn, Germany;
Grant Comer, MD, University of Michigan, Kellogg Eye Center, Ann Arbor, MI (USA);
Barbara Blodi, MD, University of Wisconsin, Madison, WI (USA);
Diana Do, MD, The Wilmer Eye Institute, Baltimore, MD (USA);
Alexander Brucker, MD, Scheie Eye Institute, Philadelphia, PA (USA);
Raja Narayanan, MD, LV Prasad Eye Institute, Hyderabad, India;
Sebastian Wolf, MD, PhD, University of Bern, Bern, Switzerland;
Philip Rosenfeld, MD, PhD, Bascom Palmer, Miami, FL (USA);
Paul S. Bernstein, MD, PhD, Moran Eye Center, University of Utah, UT (USA);
Joan W. Miller, MD, Massachusetts Eye and Ear Infirmary, Harvard Medical School, Boston, MA (USA)